4.2.4 Chemical Diffusion Coefficient

By combining the effect of the thermodynamic biasing with the results we found by examining the Kirkendall effect of the moving atomic planes we can find the chemical interdiffusion coefficient $\tilde{D}$ with which we can describe the intermixing of two constituents which form a nonideal solution. Recall our expression for $\tilde{D}$:

$$\tilde{D} = x_A \tilde{D}_B + x_B \tilde{D}_A$$

where $\tilde{D}_A$ and $\tilde{D}_B$ are the intrinsic diffusivites of the two components. We can find a relationship between the thermodynamic biasing of these diffusivities by using the Gibbs-Duhem relation:

$$x_A d\mu_A + x_B d\mu_B = 0 \tag{4.12}$$

Looking at our expression for μ:

$$\mu_A = \mu_0 + k_B T \ln a_A = \mu_0 + k_B T \left(\ln x_A + \ln \gamma_A\right)$$

we find:

$$\begin{aligned} x_A d\mu_A &= k_B T \left(dx_A + x_A d \ln \gamma_A\right) \\ &= k_B T \left(1 + \frac{\partial \ln \gamma_A}{\partial \ln x_A}\right) dx_A \end{aligned}$$

Plugging this into the Gibbs-Duhem relation (Eqn 4.12) we find:

$$k_B T \left(1 + \frac{\partial \ln \gamma_A}{\partial \ln x_A}\right) dx_A + k_B T \left(1 + \frac{\partial \ln \gamma_B}{\partial \ln x_B}\right) dx_B = 0$$

And since $dx_A = -dx_B$ we can find that:

$$\frac{\partial \ln \gamma_A}{\partial \ln x_A} = \frac{\partial \ln \gamma_B}{\partial \ln x_B}$$

Plugging Eqn. 4.11 into our expression for the chemical diffusivity, $\tilde{D}$, and using the above relation, we find:

$$\begin{aligned}\tilde{D} &= \tilde{D}_A x_B + \tilde{D}_B x_A \\ &= D_A x_B \left(1 + \frac{\partial \ln \gamma_A}{\partial \ln x_A}\right) + D_B x_A \left(1 + \frac{\partial \ln \gamma_B}{\partial \ln x_B}\right) \\ &= (D_A x_B + D_B x_A) \left(1 + \frac{\partial \ln \gamma_A}{\partial \ln x_A}\right)\end{aligned}$$

This is our final expression relating the chemical diffusivity, $\tilde{D}$, which is a measure of how a diffusion couple intermixes and is defined by Fick's laws, and the tracer diffusivities, D_i, which measure the interdiffusion of dilute or ideal solutions, and the non-ideality of the solution represented by the activity coefficient, γ_i.

4.2.5 Regular Solution Example

As an example of the thermodynamic driving force for diffusion, we consider a regular solution of N atoms, where the entropy of mixing is given by the ideal solution mixing entropy:

$$\Delta S_{mix} = -k_B N \left(x_A \ln x_A + x_B \ln x_B\right)$$

and the non-ideality of the solution is represented by the enthalpy of mixing, which in the quasichemical approximation is given by:

$$\Delta H_{mix} = x_A x_B n \Omega^{\mathrm{RS}}$$

where Ω^{RS} is a measure of the strength of unlike bonds, and is given by:

$$\Omega^{\mathrm{RS}} = z \left[H_{AB} - \frac{1}{2}\left(H_{AA} + H_{BB}\right)\right]$$

where z is the number of nearest neighbors, n is the total number of moles of atoms, and H_{ij} is the bond enthalpy per mole for $i - j$ bonds. Here the bonding enthalpy is negative for a stable bond, so the enthalpy of mixing ΔH_{mix} is negative for systems where the A-B bond is stable relative to A-A and B-B bonds.

It can be shown that in this case, Darkens equation for the chemical diffusivity:

$$\tilde{D} = (D_A x_B + D_B x_A)\left(1 + \frac{d\ln\gamma_A}{d\ln x_A}\right)$$

can be written as :

$$\tilde{D} = (D_A x_B + D_B x_A)\left(1 - \frac{2\Delta H_{\text{mix}}}{k_B T}\right)$$

where ΔH_{mix} is the mixing enthalpy per atom. The free energy, activity, and diffusion enhancement are shown for two cases in Figs. 4.1 and 4.2.

4.3 Potential Gradients and Jump Frequencies

The increase in intermixing for solutions with a negative heat of mixing is an example of diffusion in the presence of a driving force. We have seen that in general the diffusive flux will reflect gradients in other potentials as well, and is given by Eqn. 4.6:

$$J_i = -\sum_k M_{ik}\frac{d\mu_k}{dz} - M_{iT}\frac{dT}{dz} - M_{iP}\frac{dP}{dz} - M_{i\phi}\frac{d\phi}{dz}$$

We also have found that the mobility M_{ii} is related to the tracer diffusivity D_i through:

$$M_{ii} = \frac{c_i D_i}{k_B T}$$

where D_i is just the tracer diffusion coefficient of i which is the diffusivity in the absence of driving forces. In order to examine the atomistic behavior in the presence of a driving force, we consider the energetics of a biased atomic jump. Figure 4.3 shows a schematic of the energy of an atom as a function of its position during a jump from one lattice site to another which results in lowering of its energy due to traveling down a potential gradient. The amount its energy is lowered is just $-\nabla\phi\Delta z$ where ϕ is the potential of the atom, and Δz is the difference in position between the two lattice sites. In a potential with a gradient, the atom will experience a force $F = -\nabla\phi$, and in terms of this, the energy drop is $F\Delta z$.

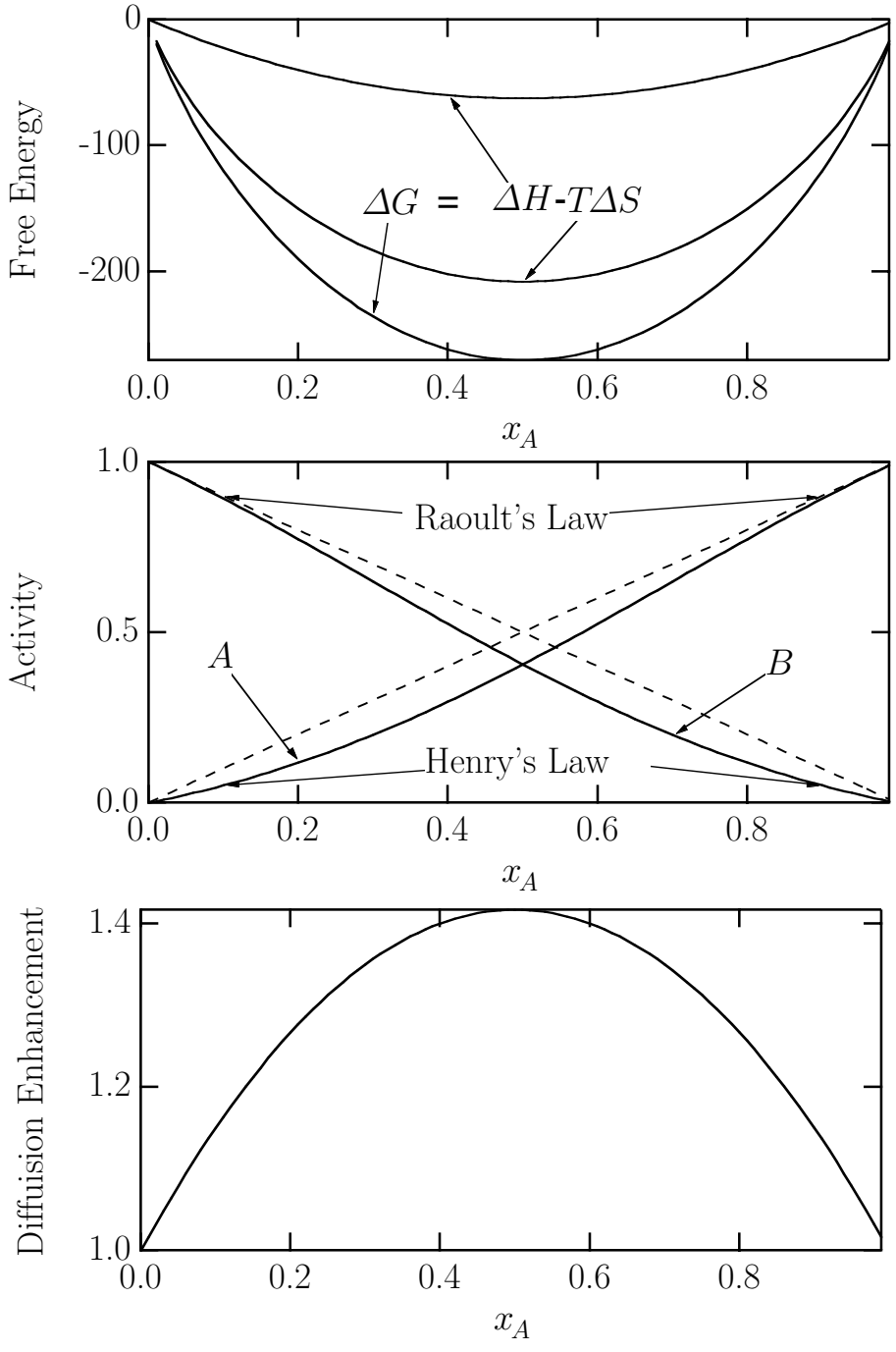

Figure 4.1: Free energy, activity, and diffusion enhancement for regular solution theory in the quasichemical approximation for the case of $\Omega^{\rm RS} = -250$K.

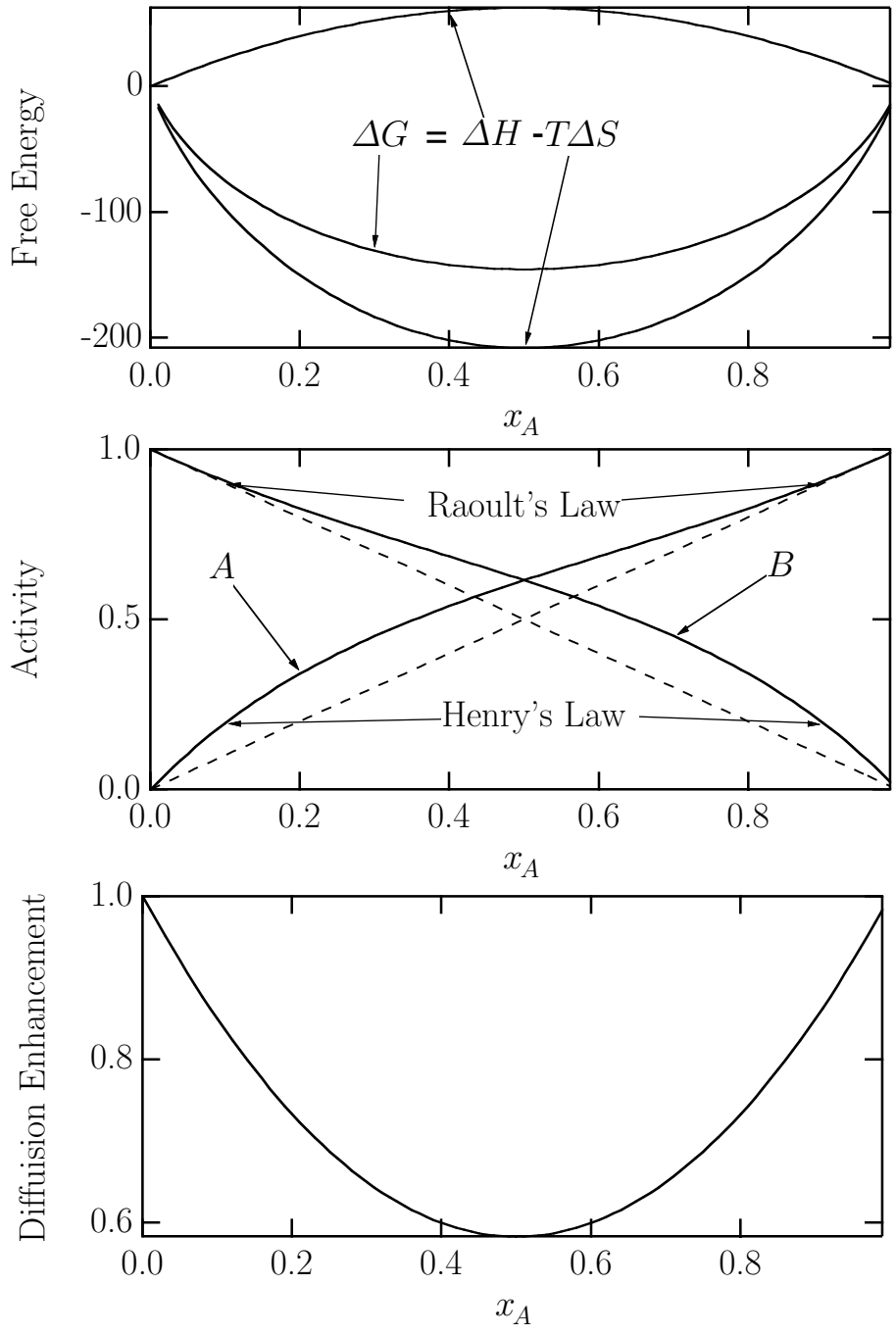

Figure 4.2: Free energy, activity, and diffusion enhancement for regular solution theory in the quasichemical approximation for the case of $\Omega^{\mathrm{RS}} = 250\mathrm{K}$.

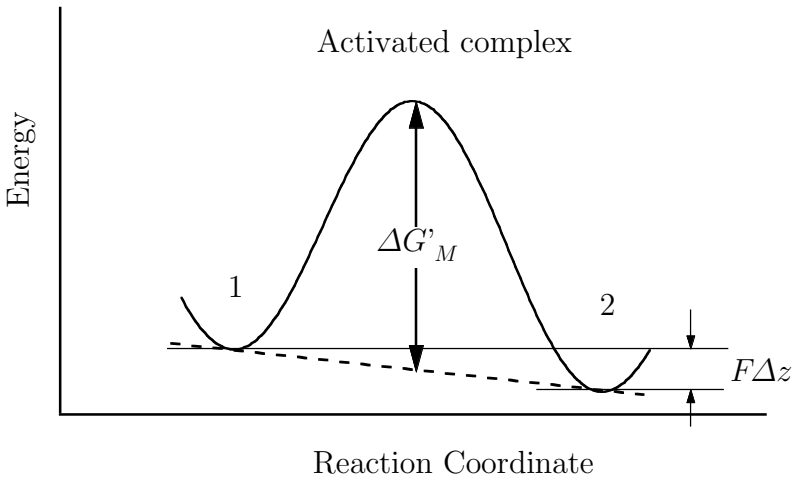

Figure 4.3: Schematic of the energy of an atom during a biased atomic jump.

The jump frequencies in the two directions will no longer be equal since the barrier as seen going from left to right is less than that seen going from right to left. In the forward direction the rate of exchange is:

$$\begin{aligned} \nu_+ &= \nu_0 \exp\left(-\frac{\Delta G'_M}{k_B T} - \frac{\nabla\phi\Delta z}{2k_B T}\right) \\ &= \nu_0 \exp\left(-\frac{\Delta G'_M}{k_B T}\right) \exp\left(\frac{-\nabla\phi\Delta z}{2k_B T}\right) \\ &\approx \nu\,(1+\epsilon) \end{aligned} \tag{4.13}$$

while in the reverse direction it is:

$$\begin{aligned} \nu_- &= \nu_0 \exp\left(-\frac{\Delta G'_M}{k_B T} + \frac{\nabla\phi\Delta z}{2k_B T}\right) \\ &= \nu_0 \exp\left(-\frac{\Delta G'_M}{k_B T}\right) \exp\left(\frac{\nabla\phi\Delta z}{2k_B T}\right) \\ &\approx \nu\,(1-\epsilon) \end{aligned} \tag{4.14}$$

where ν is the exchange rate in the absence of a potential gradient given by:

$$\nu = \nu_0 \exp\left(-\frac{\Delta G'_M}{k_B T}\right)$$

and ϵ is change in exchange rate due to the potential gradient and to first order is given by:

$$\epsilon = -\frac{\nabla\phi\Delta z}{2k_BT} = \frac{F\Delta z}{2k_BT} \tag{4.15}$$

where $F = -\nabla\phi$ is the driving force for atomic motion.

In order to see how this affects diffusion, we consider the simple one-dimensional case we examined Section 1.2.1. We calculate the net flux of atoms to the right by taking the difference between the total fluxes in the two directions. We have:

$$J = J_+ - J_- = \Gamma_+\sigma(z) - \Gamma_-\sigma(z+\Delta z) \tag{4.16}$$

where $\sigma(z)$ is the planar atomic density at position z, Δz is the jump distance, and Γ_+ and Γ_- are the average rate a given atom jumps to the right and left respectively. The atomic jump rates are given by:

$$\Gamma_\pm = pjz_{nn}\nu_\pm = pjz_{nn}\nu\ (1 \pm \epsilon) = j\Gamma\ (1 \pm \epsilon)$$

where z_{nn} is the number of nearest neighbors, j is the fraction of them in the jump direction, Γ is the average jump frequency[3], and we have used Eqns. 4.13 and 4.14. For the one-dimensional case $j = 1/2$.

Inserting this into Eqn. 4.16 we find the flux:

$$\begin{aligned}
J_i &= \frac{1}{2}\left[\Gamma\ (1+\epsilon)\ \sigma(z) - \Gamma\ (1-\epsilon)\ \sigma(z+\Delta z)\right] \\
&= \frac{1}{2}\left\{\Gamma\ \left[\sigma(z) - \sigma(z+\Delta z)\right] + \Gamma\epsilon\ \left[\sigma(z) + \sigma(z+\Delta z)\right]\right\} \\
&= \frac{-\Gamma}{2}\left(\Delta z\right)^2 \frac{c_i(z+\Delta z) - c_i(z)}{\Delta z} + \Gamma\epsilon c_i(z)\Delta z \\
&= \frac{-\Gamma}{2}\left(\Delta z\right)^2 \frac{\partial c_i}{\partial z} - \frac{\Gamma}{2}(\Delta z)^2 \frac{c_i\nabla\phi}{k_BT} \\
&= -D_i\frac{\partial c_i}{\partial z} - \frac{D_ic_i\nabla\phi}{k_BT} \\
&= -D_i\frac{\partial c_i}{\partial z} + \frac{D_ic_iF}{k_BT}
\end{aligned}$$

where we have identified $D = \frac{1}{2}\Gamma(\Delta z)^2$ as before.

[3]In general Γ is given by $\Gamma = pz\nu$.

We see that the effect of the potential gradient is to add to the flux a term which is proportional to the driving force. By comparison with Eqn. 4.6 we can identify the mobility $M_{i\phi}$ as:

$$M_{i\phi} = \frac{c_i D_i}{k_B T}$$

4.3.1 Chemical Potential as Driving Force

We can see that for a nonideal solution, gradients in chemical potential also give rise to an effective driving force. The chemical potential is given by:

$$\begin{aligned} \mu_i &= \mu_{0i} + k_B T \ln a_i \\ &= \mu_{0i} + k_B T (\ln \gamma_i + \ln x_i) \\ &\equiv \mu_i' + k_B T \ln x_i \end{aligned}$$

where μ_i' accounts for all the nonidealities of the solution. In the absence of other potential gradients, the flux becomes:

$$\begin{aligned} J_i &= -M_{ii} \frac{\partial \mu_i}{\partial z} \\ &= -c_i D_i \frac{\partial \ln x_i}{\partial z} - \frac{c_i D_i}{k_B T} \frac{\partial \mu_i'}{\partial z} \\ &= -D_i \nabla c_i - \frac{D_i c_i \nabla \mu_i'}{k_B T} \end{aligned}$$

So we see that a gradient in the ideal part of the chemical potential gives rise to the normal Fick's law diffusive flux, while a gradient in the nonideal part plays the role of a potential gradient and gives rise to an effective driving force. We can account for this change by using the intrinsic diffusivities $\tilde{D}$ in Fick's laws.

4.4 Vacancy Equilibrium and Kirkendall Voids

One interesting consequence of the difference in diffusivities for two constituents in a diffusion couple, is the flux of vacancies. Recall that we have asserted that in the bulk of the crystal, there is no destruction or creation of lattice sites, that is:

$$J_A + J_B + J_V = 0$$

Therefore, the vacancy flux, given by:

$$J_V = -J_B - J_A = \tilde{D}_B \frac{\partial c_B}{\partial z} + \tilde{D}_A \frac{\partial c_A}{\partial z} = \left(\tilde{D}_B - \tilde{D}_A\right) \frac{\partial c_B}{\partial z}$$

will be non zero if $\tilde{D}_B \neq \tilde{D}_A$. That is, there must be a net vacancy flux to accommodate the differences in the fluxes of the constituents.

Recall also that we have assumed that the vacancy concentration was everywhere equal to the equilibrium value, so that:

$$\frac{\partial c_V}{\partial t} = 0$$

If we apply the conservation equation to the vacancy concentration we find:

$$\frac{\partial c_V}{\partial t} = -\frac{\partial J_V}{\partial z} + \dot{c}_V = 0$$

where $\dot{c}_V$ is the vacancy source term, which is the rate of destruction or creation of vacancies. We see that in order to maintain the difference in fluxes while maintaining the equilibrium vacancy concentration, we must have a vacancy source term given by:

$$\dot{c}_V = \frac{\partial J_V}{\partial z} = -\frac{\partial J_A}{\partial z} - \frac{\partial J_B}{\partial z}$$

An example of this situation is shown in Fig. 4.4 where we have taken the composition profile calculated numerically using the methods of Section 1.7.2. We assume that the diffusivity depends linearly on composition:

$$\tilde{D} = x_A \tilde{D}_B + x_B \tilde{D}_A = x_B \left(\tilde{D}_A - \tilde{D}_B\right) + \tilde{D}_B = ac + b$$

where $c = x_B/V_m$, is the composition of B, V_m is the atomic volume, $a = V_m \left(\tilde{D}_A - \tilde{D}_B\right)$ is a measure of the difference in diffusivities, and $b = \tilde{D}_B$. We developed the numerical methods for solving this equation before we had any justification for this particular form of the diffusivity, but we are now in a position to see how this can arise. For a and b to be constant, the thermodynamic driving force must be neglegible so that $\tilde{D}_A = D_A$ and $\tilde{D}_B = D_B$, and both D_A and D_B must be independent of composition. The composition profile in Fig. 4.4 is calculated assuming $D_A = 10 D_B$.

We see immediately that the flux of vacancies plays an important role in the diffusion. There are regions where vacancies must be created or destroyed

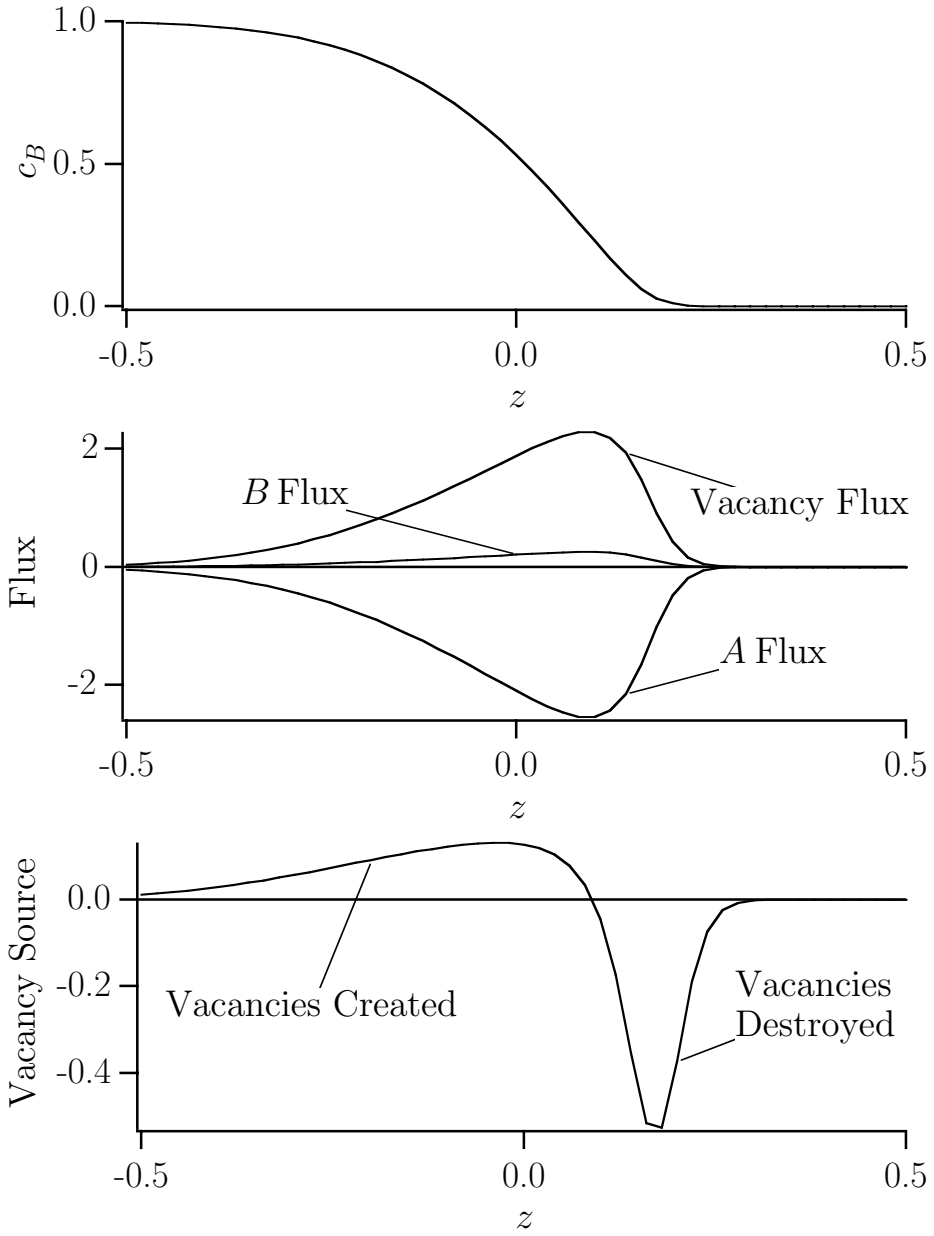

Figure 4.4: Calculated concentration profile, fluxes, and vacancy source term for the case where $\tilde{D}_A > \tilde{D}_B$.

to maintain this flux in the face of the requirement of maintaining the equilibrium concentration of vacancies. For example, in some regions of the sample, the concentration of A atoms is diminishing faster than the concentration of B atoms is increasing. In these regions there is a positive accumulation of vacancies to balance out this difference in concentration changes. However, since the concentration of vacancies is maintained at its equilibrium value, there must be a vacancy sink which consumes this vacancy accumulation. Hence there are regions of the sample where vacancies are destroyed.

We have an apparent contradiction, on one hand, we say that there are no lattice sites being created or destroyed, and on the other, we see that there must be a vacancy source term to maintain the equilibrium concentration. The answer lies in the spatial distribution of the vacancy sources and sinks. We say that inside a grain, away from defects, there can be no vacancy creation or annihilation, so lattice sites are conserved. However, we imagine that there are vacancy sources and sinks close enough so that the equilibrium concentration can be maintained. Vacancies can be created or destroyed at any number of crystal defects, including grain boundaries, surfaces, and dislocations. Generally surfaces and grain boundaries are not distributed evenly enough to maintain the equilibrium concentration of vacancies, and edge dislocations are moved out of a given region by a vacancy flux. However a combination dislocation with a screw component along the diffusion direction and an edge component perpendicular to the flux will rotate in response to a vacancy flux and produce a plane of vacancies with each rotation.

Of course, there must be a thermodynamic driving force in order for the sources or sinks to produce or annihilate vacancies. This driving force comes from nonequilibrium concentrations of vacancies. In the case of an excess concentration, vacancies are being destroyed, and in fact they can precipitate out to form voids, known as Kirkendall voids. These voids form in the region labeled "vacancies destroyed" in Fig. 4.4.

4.5 The Kirkendall Experiment

In a classic study of diffusion in CuZn alloys, Kirkendall and Smigelskas used measurements of marker velocity and diffusivity to find the diffusivities of Cu and Zn. As a summary of the material in this chapter, we consider analysis of this experiment. A $Cu_{0.7}Zn_{0.3}$ bar was wound with thin W marker wire and

then coated with pure Cu by electrodeposition. During anneals they found the markers position moved by an amount proportional to the square root of time ($z_m = \alpha\sqrt{t}$), staying at a concentration of 22.5 % Zn. By applying Boltzmann-Matano analysis to the composition profile obtained after anneals they were able to measure the chemical diffusivity $\tilde{D}$. Using the equations

$$v = \frac{dz_m}{dt} = \frac{\alpha}{2\sqrt{t}} = \frac{z_m}{2t} = \left(\tilde{D}_{\rm Zn} - \tilde{D}_{\rm Cu}\right)\frac{1}{c}\frac{\partial c_{\rm Zn}}{\partial z}$$

and

$$\tilde{D} = x_{\rm Cu}\tilde{D}_{\rm Zn} + x_{\rm Zn}\tilde{D}_{\rm Cu}$$

they were able to find the diffusivities of Cu and Zn at $T = 1058$ K:

$$\begin{aligned} \tilde{D}_{\rm Zn} &= 5.1 \times 10^{-9}\ {\rm cm}^2/{\rm s} \\ \tilde{D}_{\rm Cu} &= 2.2 \times 10^{-9}\ {\rm cm}^2/{\rm s} \end{aligned}$$

Hence the ratio of diffusivities of Zn to Cu is

$$\frac{\tilde{D}_{\rm Zn}}{\tilde{D}_{\rm Cu}} = 2.3$$

Further, independent measurements of the diffusivity of Zn at low concentrations yielded

$$\frac{\tilde{D}_{\rm Zn}(22.5\%)}{\tilde{D}_{\rm Zn}(0)} = 17$$

To examine the reasons behind the behavior diffusivities of Cu and Zn in the Kirkendall experiments we consider the probability factors for the two species. It is first helpful to calculate the fraction g of the Zn atoms involved in vacancy-impurity pairs. Recall our expression for the number fraction of vacancy-impurity pairs:

$$x^0_{IV} = \frac{z x_{It} \exp\left[-\left(\Delta G_B + \Delta G'_V\right)/k_B T\right]}{1 + z\exp\left[-\left(\Delta G_B + \Delta G'_V\right)/k_B T\right]}$$

Hence the fraction of impurities associated with a vacancy is

$$g \equiv \frac{x^0_{IV}}{x_{It}} = \frac{z\exp\left[-\left(\Delta G_B + \Delta G'_V\right)/k_B T\right]}{1 + z\exp\left[-\left(\Delta G_B + \Delta G'_V\right)/k_B T\right]}$$

Note that g has the limits

$$\begin{aligned} g &\approx zx_V^0 \text{ for } \Delta G_B = 0 \text{ and} \\ g &\approx 1 \text{ for } \Delta G_B < 0 \text{ and } |\Delta G_B| \gg \Delta G'_V \end{aligned}$$

The probability $p_{\rm Zn}$ that a given lattice site next to a Zn atom is vacant is a sum the probability that the Zn atom is involved in a vacancy-impurity pair divided by the number of nearest neighbors, plus the number of extra vacancies added due to the vacancy-impurity interaction.

$$p_{\rm Zn} = \frac{g}{z} + (g - zx_V^0)x_{It}$$

Note that this has the limits

$$\begin{aligned} p_{\rm Zn} &\approx x_V^0 \text{ for } \Delta G_B = 0 \text{ and} \\ p_{\rm Zn} &\approx \frac{1}{z} + x_{It} \text{ for } \Delta G_B < 0 \text{ and } |\Delta G_B| \gg \Delta G'_V \end{aligned}$$

Similarly the probability $p_{\rm Cu}$ that a given lattice site next to a Cu atom is:

$$p_{\rm Cu} = x_V^0 + (g - zx_V^0)x_{It}$$

has the limits

$$\begin{aligned} p_{\rm Cu} &\approx x_V^0 \text{ for } \Delta G_B = 0 \text{ and} \\ p_{\rm Cu} &\approx x_V^0 + x_{It} \text{ for } \Delta G_B < 0 \text{ and } |\Delta G_B| \gg \Delta G'_V \end{aligned}$$

Hence the ratio of probabilities $p_{\rm Zn}/p_{\rm Cu}$ goes from 1 to $1 + 1/zx_{It}$ as ΔG_B goes from 0 to $-\infty$. For the system with 22.5 Zn, this maximum value is 1.37. Using $\Delta G_B = -0.1$ eV and

$$\begin{aligned} \Delta G'_V &\approx \Delta H_V^{\rm Cu} \frac{T_M^{\rm CuZn}}{T_M^{\rm Cu}} \\ &= 1.29 \frac{1236}{1358} \\ &= 1.17 \text{ eV} \end{aligned}$$

we find

$$\frac{p_{\rm Zn}}{p_{\rm Cu}} = 1.31.$$

Interestingly, although only one in 10,000 Zn atoms is bound to a vacancy ($g \approx 10^{-4}$), the effect on the relative probabilities $p_{\rm Zn}/p_{\rm Cu}$ of these vacancies is almost at its maximum value. The Zn atoms do see more vacancies than Cu atoms but not the factor of 2.3 which is the observed ratio of the diffusivities. We don't want to push our simple model too far, but we might conclude that the correlation factor might be greater for the Zn atoms to account for this difference. In fact we can see that there are about 8 times as many vacancy-impurity pairs than there are free vacancies ($x^0_{IV}/x^0_V \approx 8$), so that most of the diffusion occurs by motion vacancies attached to the Zn atoms, and the attractive interaction between vacancies and the Zn impurities greatly enhances diffusion.

We next try to understand the 17-fold increase in the diffusivity of Zn as the alloy fraction is increased from 0 to 22.5%. The increase in number fraction of free vacancies is given by

$$\frac{x^0_V({\rm CuZn})}{x^0_V({\rm Cu})} = \frac{\exp(-1.17/k_BT)}{\exp(-1.29/k_BT)} \approx 3.7$$

So there are almost four times as many free vacancies in the alloy due to the lowering of the melting temperature and the associated lowering of the energy cost of vacancy formation.

However, the vacancies associated with the vacancy-impurity pairs also play a role in diffusion. If we calculate the ratio of the probabilities that a given neighbor of a Zn atom is vacant in the alloy relative to that of Zn in pure Cu, we find

$$\frac{p^{\rm CuZn}_{\rm Zn}}{p^{\rm Cu}_{\rm Zn}} = \frac{g^{\rm CuZn}/z + (g^{\rm CuZn} - zx^0_V)x_{It}}{g^{\rm Cu}/z} \approx 10.4$$

This is pretty good agreement with the observed factor of 17 increase in the Zn diffusivity. Again we might conclude that the difference between our simple model and the observed diffusivities is due to a difference in the correlation factor.